

**Monte Carlo Calculations Using MCNP4B for an Optimal Shielding Design  
of a 14-MeV Neutron Source\***

James C. Liu and Tony T. Ng

Stanford Linear Accelerator Center  
MS 48, P.O. Box 4349  
Stanford, CA 94309, USA

Submitted to the Journal of Radiation Protection Dosimetry

---

\* Work supported by the Department of Energy under contract DE-A-03-76SF00515

**Abstract** - The shielding for 14-MeV neutrons from a D-T generator at SLAC needs to be optimized in terms of shield thickness and cost. Shielding calculations were made using the MCNP4B Monte Carlo code and the ENDF/B-VI cross section set. A few materials were studied: iron, borated polyethylene, three types of normal and heavy concrete, and mixtures of iron and borated polyethylene. The effects of shielding geometry (sphere, cube, and the proposed geometry) were also examined. The transmission results of ambient dose equivalents, as well as the attenuation lengths and the average energies, for neutrons and gammas outside the shielding are presented.

## Introduction

The energy calibration of the CsI detector for the BaBar detector at the Stanford Linear Accelerator Center (SLAC) requires the use of mono-energetic 14-MeV neutrons to activate the fluorinert liquid ( $C_8F_{18}$ ). Due to the space limitation, the shielding for the 14-MeV neutron source from the D-T generator needs to be optimized in terms of shielding thickness and cost. The goal is to design a shielding with a total thickness no more than two feet and a relative transmission factor of 0.004 for ambient dose equivalent. The materials that are chosen should be readily available and not expensive. NCRP72 <sup>(1)</sup> gives only that 2'-thick concrete (density  $\rho = 2.35 \text{ g cm}^{-3}$ ) and 2'-thick water would provide a dose equivalent index transmission factor of 0.02 and 0.04, respectively. Therefore, other materials need to be investigated. In this study, calculations to design the optimal shielding were performed using the MCNP4B Monte Carlo code <sup>(2)</sup> and the latest ENDF/B-VI cross section set.

## Methods

For the shielding optimization study, shielding using a single material were first analyzed. Materials that were studied included iron ( $\rho = 7.86 \text{ g cm}^{-3}$ ), 10% wt borated polyethylene (BPE,  $\rho = 0.96 \text{ g cm}^{-3}$ ), and three types of concrete: ANSI concrete ( $\rho = 2.35 \text{ g cm}^{-3}$ , 5.04% wt  $H_2O$ ) <sup>(3)</sup>, heavy concrete XN244 ( $\rho = 3.85 \text{ g cm}^{-3}$ ), and heavy concrete XN280 ( $\rho = 4.62 \text{ g cm}^{-3}$ ). Actual, but confidential, composition of the two types of heavy concrete (normal concrete added with iron) were provided by the manufacturer (Atomic International Inc. #). Shielding using a

---

# Atomic International Inc., P.O. Box 279, Frederick, PA, 19435, USA

combination of two materials, iron followed by BPE or BPE followed by iron, were also analyzed. The D-T generator tube will be immersed in a fluorinert liquid ( $C_8F_{18}$ ,  $\rho = 1.8 \text{ g cm}^{-3}$ ) and, therefore, the self-shielding effect of the liquid was also examined.

For better statistics, a spherical shielding geometry was used in the MCNP4B geometry simulation with an isotropic 14-MeV neutron source located in the origin. Surrounding the point source is a 20-cm-thick layer of vacuum or the fluorinert liquid, followed by the shielding materials and, then, a fluence-scoring sphere surface at 200 cm away from the origin. For comparison purpose, a cubical geometry with shields of fluorinert followed by iron and then BPE was also studied. In this case, a point detector at 100 cm away from the center of the cube, at which the point isotropic neutron source is located, was used. Finally, a shielding using the actual geometry of the D-T generate tube, the cylindrical fluorinert bath, and slab shield (iron followed by BPE) proposed by project engineer was studied with four point detectors around the shield.

The ENDF/B-VI cross section set for all elements was used in the MCNP4B calculations. Thermal neutrons were transported to ensure proper production of gammas. The fluence to ambient dose equivalent conversion factors for neutrons and photons from ICRP74<sup>(4)</sup> were used. The relative transmission is simply the ratio of the ambient dose equivalent values (neutron or gamma) with shield and the neutron ambient dose equivalent without shield. All calculated transmission factors had a standard deviation less than 5%.

## Results and Discussions

### Spherical Shielding Geometry

#### *Iron or BPE Shield*

For a spherical shield of iron or BPE up to 2'-thick, Fig. 1a shows that the ambient dose equivalent is dominated by neutrons (over 99% for iron and 90% for BPE). Iron shield of 2'-thick provides only a relative transmission of 0.05 for total dose equivalent, while 2'-thick BPE gives a much lower transmission factor of 0.0053 (neutron 0.0049, gamma 0.0004). The attenuation length  $\lambda$  for neutrons (and also for total dose equivalent in this case) reaches its equilibrium value of  $278 \text{ g cm}^{-2}$  (14") for iron and  $13 \text{ g cm}^{-2}$  (5.3") for BPE.

The average energies of the neutron and gamma spectra outside the shield are shown in Fig. 1b. For iron shield, the neutron average energy decreases quickly and approaches an asymptotic value of 0.2 MeV (near iron's resonant region). This is because that the high inelastic cross section of iron causes fast neutrons to slow down rapidly until neutrons are below resonant region, and the elastic cross section in iron is not effective in reducing the energies of slow neutrons. On the other hand, the average neutron energy in BPE decreases slowly and flattens out to 7.5 MeV at two feet.

It is worth to compare the attenuation length of gamma in iron ( $482 \text{ g cm}^{-2}$  in Fig. 1a) with its associated average gamma energy ( $\sim 2 \text{ MeV}$  in Fig. 1b). The gammas produced from the inelastic or capture reaction of neutrons with iron are attenuated by iron itself. Traditionally, the attenuation length can be obtained from both the attenuation coefficient and the build-up factor. If the build-up factor is not known, the attenuation length can be estimated to be the inverse of the mass energy absorption coefficient. Therefore, using a gamma energy of 2 MeV, the attenuation length in iron is estimated to be  $46 \text{ g cm}^{-2}$ , which is much smaller than the MCNP-calculated value

of  $482 \text{ g cm}^{-2}$ . Even with an attenuation coefficient of  $0.042 \text{ cm}^2 \text{ g}^{-1}$  and a conservative build-up factor of  $10^{(4)}$ , the estimated attenuation length is still less than the MCNP value. The reason for this difference is due to the fact that, in the 14-MeV neutron case, the gammas are attenuated in iron but, at the same time, the gammas are also replenished from the neutron interaction with iron. This is in contrast to the traditional case where only gammas are incident on and attenuated in the shield without replenishment. Thus, the gamma attenuation length in this case is “controlled” by neutrons and is much larger than the estimated one in traditional case.

For 10% borated polyethylene, neutrons are mainly slowed down by the elastic cross section of hydrogen and then captured by boron. Most gammas are produced from the neutron’s interaction with carbon and boron, instead of hydrogen. The resulting gamma spectrum has an average energy of 0.9 MeV (Fig. 1b) and an attenuation length of  $33 \text{ g cm}^{-2}$  (Fig. 1a). Note that, in ordinary polyethylene without boron, thermalized neutrons would generate a captured gamma spectrum with a higher average energy of 2.2 MeV from the  ${}^1\text{H}(n,\gamma){}^2\text{H}$  reaction.

### *Concrete Shield*

Figure 2a shows the relative transmission of neutron, gamma, and total ambient dose equivalents in ANSI concrete and heavy concrete (XN240 and XN288) up to 4’-thick. Figure 2b shows the average energies of the neutron and gamma spectra outside all types of concrete shields approach the same equilibrium values of 0.9 MeV and 2 MeV, respectively.

Again, neutrons dominate the dose equivalent outside all concrete shields, particularly for heavy concrete in which the added iron provides more gamma attenuation. At the desired 2’-thickness, the transmission factors provided by ANSI concrete, XN240, and XN288 are 0.0094, 0.0036, and 0.0027, respectively. Therefore, 2’-thick XN240 or XN288 can meet the shielding

design goal of 0.004. The transmission factor of 2'-thick ANSI concrete is a factor of 2 lower than the NCRP value <sup>(1)</sup>, due to the difference in the first Tenth Value Layer.

The equilibrium attenuation length  $\lambda$  for neutrons is 36 g cm<sup>-2</sup> (6") for ANSI concrete, 44 g cm<sup>-2</sup> (4.5") for XN240, and 49 g cm<sup>-2</sup> (4.2") for XN288. The equilibrium  $\lambda$  value for the ANSI concrete agrees with those in references <sup>(1,5)</sup>, considering the differences in the method, geometry, and/or cross section used in the calculations. Because normal concrete already has a mixture of light and heavy elements, heavier concrete with more iron actually has a lower neutron attenuation capability (per unit mass thickness). As expected, the gamma attenuation length in units of mass thickness is the same for ANSI concrete, XN240, and XN288, and it is 52 g cm<sup>-2</sup>.

### *Iron-BPE Shield*

Figure 1a shows that using 2'-thick iron or BPE alone would not meet the design goal of a transmission factor of 0.004. However, a shield with both iron and BPE could be more effective than just iron or BPE alone, because the advantages of both iron and BPE are utilized. Iron is effective in slowing down high-energy neutrons (e.g., 14-MeV source neutrons) and attenuating gammas, while hydrogen of BPE is effective in slowing down fast neutrons (a few MeV), and <sup>10</sup>B has a high absorption cross section for thermal neutrons and a low production yield of gammas.

The question is then which (and how much) should be put closer to the neutron source to balance the neutron and gamma dose components such that the minimum of total dose equivalent can be obtained. At accelerator facilities like SLAC, it is well known to put heavy metal closer to the high-energy neutron source. It has also been shown <sup>(6)</sup> that, for <sup>252</sup>Cf neutrons, putting stainless steel in front of polyethylene is better in reducing the total dose equivalent. Therefore, it seems that, for 14-MeV neutrons, the iron shield should be positioned first, followed by BPE.

Figure 3a shows that a shield of 1' iron followed by 1' BPE (denoted as the curve of Fe+BPE at  $268.8 \text{ g cm}^{-2}$ ) is indeed ten times more effective than the reverse arrangement (BPE+FE). As expected, Fe+BPE has a better neutron, but a worse gamma, attenuation than BPE+Fe. The total transmission of 14-MeV neutrons in a 1'Fe+1'BPE spherical shield is 0.0045, which has a more balanced attenuation fraction between neutron (0.0034) and gamma (0.0011). Note that the shields in Fig. 3 have equal thickness of iron and BPE.

Figure 3b shows the average neutron and gamma energies outside the shield of Fe-BPE. Table 1 summarizes the attenuation length  $\lambda$  and average energy E of neutron and gamma (in equilibrium) from 14-MeV neutrons transmitted in a spherical shield. Note that the equilibrium neutron energy outside the Fe+BPE is higher than that outside an iron shield (7.5 MeV vs. 0.2 MeV). The spectrum hardening is caused by the preferential removal of slow neutrons in BPE.

Although the attenuation by 1'Fe+1'BPE is much better than 2'-thick iron, it is only slightly better than 2'-thick BPE. However, by varying the thickness ratio between iron and BPE (see Table 2), a total transmission factor of 0.0033 can be accomplished using 16"Fe+8"BPE. Table 2 also shows that the addition of boron to replace the neutron capture by hydrogen has a large effect on the reduction of gamma dose, but not on neutron dose (5% borated polyethylene or pure polyethylene actually is slightly better than 10% borated polyethylene). Inclusion of lead also reduces the iron-produced gamma dose significantly, as seen in Table 2.

Figure 3a also shows that the 20-cm-radius fluorinert bath, in which the neutron source was immersed, reduces the dose equivalent transmission by a factor of 2-3. As expected, the effect of the fluorinert liquid on the reduction of the average neutron energy is more pronounced when the shield of iron and BPE is thinner, but the average gamma energy is not affected (as seen in Fig. 3c).



### Cubical Shielding Geometry

A sphere is an idealized shielding geometry. To check the geometry effect, a shielding of Fe+BPE in a more reasonable cubical geometry with a point isotropic neutron source at the center of the cube (immersed in a 20-cm-thick fluorinert bath) was examined. The comparison in Fig. 4a shows that a cubical shield has a 5%-20% higher ambient dose equivalent transmission than a spherical shield (the difference becomes larger when shield becomes thicker). This is because that, in a cubical shield, there is scattering from the corners of the cube to the detector, which in this case is located near the outer surface of the shield. Because of this extra scattering, the average neutron energy in a cubical shield is also lower than that in a spherical shield by ~5% (see Fig. 4b). However, the average gamma energy outside a cubical shield was ~6% higher. As a first-order approximation in the shielding design, the transmission curve for a spherical shield can be used for a cubical shield.

### Proposed Shielding Geometry

The proposed shielding geometry with a detailed dimension is shown in Fig. 5a, in which the 14-MeV neutrons were emitted isotropically from the bottom center of a cylindrical D-T generator tube (simulated with iron with a density of  $0.5 \text{ g cm}^{-3}$ ). The tube is immersed in the fluorinert liquid inside a cylindrical iron container. The shielding (iron followed by BPE) has equal thickness on four sides of the source, except the floor and wall sides (simulated with 1'-thick concrete slab).

Four point detectors (see the coordinates of D1-D4 in Fig. 5a) were utilized. Detector D3, representing a person standing close to shielding at an appropriate height, is the main one to be

calculated. Detector D1 was used to examine the distance effect, as compared to D3. Detectors D2 and D4 were used to check the scattering effect of floor and wall.

Figures 5b-5d show the transmission curves for neutron, gamma, and total ambient dose equivalents, respectively, at detector locations D1, D3 and D4, compared with those for a spherical shield (curves  $C_8F_{18}+Fe+BPE$  from Fig. 3a). As expected, the difference among all three detectors becomes larger when the shield is thicker. The slant thickness of the shield between source and detector D3 is the largest and, thus, detector D3 has the smallest transmission among all three detectors. With a slab shield of 1'Fe+1'BPE, the total dose equivalent transmission at D3 is as low as 0.0012 (neutron 0.0004 and gamma 0.0008), which is better than a spherical shield. On the other hand, detector D4 has the smallest shield thickness and more floor scattering and, therefore, has the largest transmission factor. Detector D2, not shown in Figs. 5b-5d, actually had a ~15% higher transmission than detector D4, due to the additional scattering from the wall. In any case, the surface detector in a spherical shielding geometry is closer to detector D1 in an actual shielding geometry. The transmission curve of the surface detector in a spherical shield can also be used conservatively for detector D3 in our case.

## **Conclusions**

The transmission curves of ambient dose equivalent, calculated with MCNP4B and ENDF/B-VI cross section, indicate that, within the 2'-thick shield constraint, only heavy concrete (XN240 and XN288) meet the design goal of a transmission factor of 0.004, while 2'-thick BPE nearly achieve the goal. A shield of iron followed by BPE is better than BPE followed by iron and a shield of 14"Fe+10"BPE is needed to meet the goal. The effects of the geometry used in the

calculations are small, but not negligible. The transmission factors, together with equilibrium attenuation lengths and the average energies, for neutron and gamma radiation are also presented.

## References

1. National Council on Radiation Protection and Measurements (NCRP), *Radiation Protection and Measurements for Low-Voltage Neutron Generators*, NCRP Report 72, Bethesda, MD (1983).
2. J. Briesmeister (editor), *MCNP – A General Monte Carlo Code for Neutron and Photon Transport, Version 4B*, Los Alamos National Lab., Los Alamos, NM, MCNP4B (1997).
3. Chilton, A.B., Shultis, J.K., and Faw, R.E. *Principles of Radiation Shielding*, Prentice-Hall, Inc., (1984).
4. International Commission on Radiological Protection (ICRP), *Conversion Coefficients for Use in Radiological Protection against External Radiation*, Annals of the ICRP, ICRP Publication 74, Vol. 26(3-4), Pergamen Press, (1996).
5. Cross, W.G. and Ing, H. “Spectra and dosimetry of neutrons interacting with concrete shielding”, Proceedings of IRPA Congress, Paris (1977).
6. Ueki, K., Ohashi, A., Nariyama, N., Nagayama, S., Fujita, T., Hattori, H. and Anayama, Y. “Systematic evaluation of neutron shielding effects for materials”, Nucl. Sci. and Eng. **124**, 455-464 (1996).

Table 1. Equilibrium attenuation length  $\lambda$  and average energy E of neutron and gamma from 14-MeV neutrons transmitted in a spherical shield.

Shield Material	Iron	BPE	Concrete			Fe+BPE	BPE+Fe	
			ANSI	XN240	XN288			
Density (g cm <sup>-3</sup> )	7.86	0.96	2.35	3.85	4.62	4.41*	4.41*	
$\lambda$ (g cm <sup>-2</sup> )	278	13	36	44	49	42	94	
Neutron	$\lambda$ (cm)	35	13.5	15.3	11.4	10.6	9.5	21
	E (MeV)	0.2	7.5	0.9	0.9	0.9	7.5	0.7
Gamma	$\lambda$ (g cm <sup>-2</sup> )	482	33	52	52	52	98	51
	$\lambda$ (cm)	61	34	22	13.5	11.3	22	12
	E (MeV)	2.0	0.9	2	2	2	0.4	1.5

\* Average density of iron and 10% borated polyethylene, with equal thickness of iron and BPE.

Table 2. Effects of thickness ratio between iron and BPE and addition of boron or lead.

Shield Type	Ambient Dose Equivalent Transmission		
	Neutron	Gamma	Total
8''Fe+16''BPE	0.0064	0.0012	0.0076
10''Fe+14''BPE	0.0048	0.0011	0.0059
12''Fe+12''BPE	0.0034	0.0011	0.0045
14''Fe+10''BPE	0.0024	0.0012	0.0036
16''Fe+8''BPE	0.0018	0.0015	0.0033
12''Fe+12''BPE (5% B)	0.0031	0.0012	0.0043
12''Fe+12''PE (no B)	0.0031	0.0056	0.0087
4''Pb+8''Fe+12''BPE	0.0015	0.0002	0.0017
8''Fe+4''Pb+12''BPE	0.0010	0.0001	0.0011

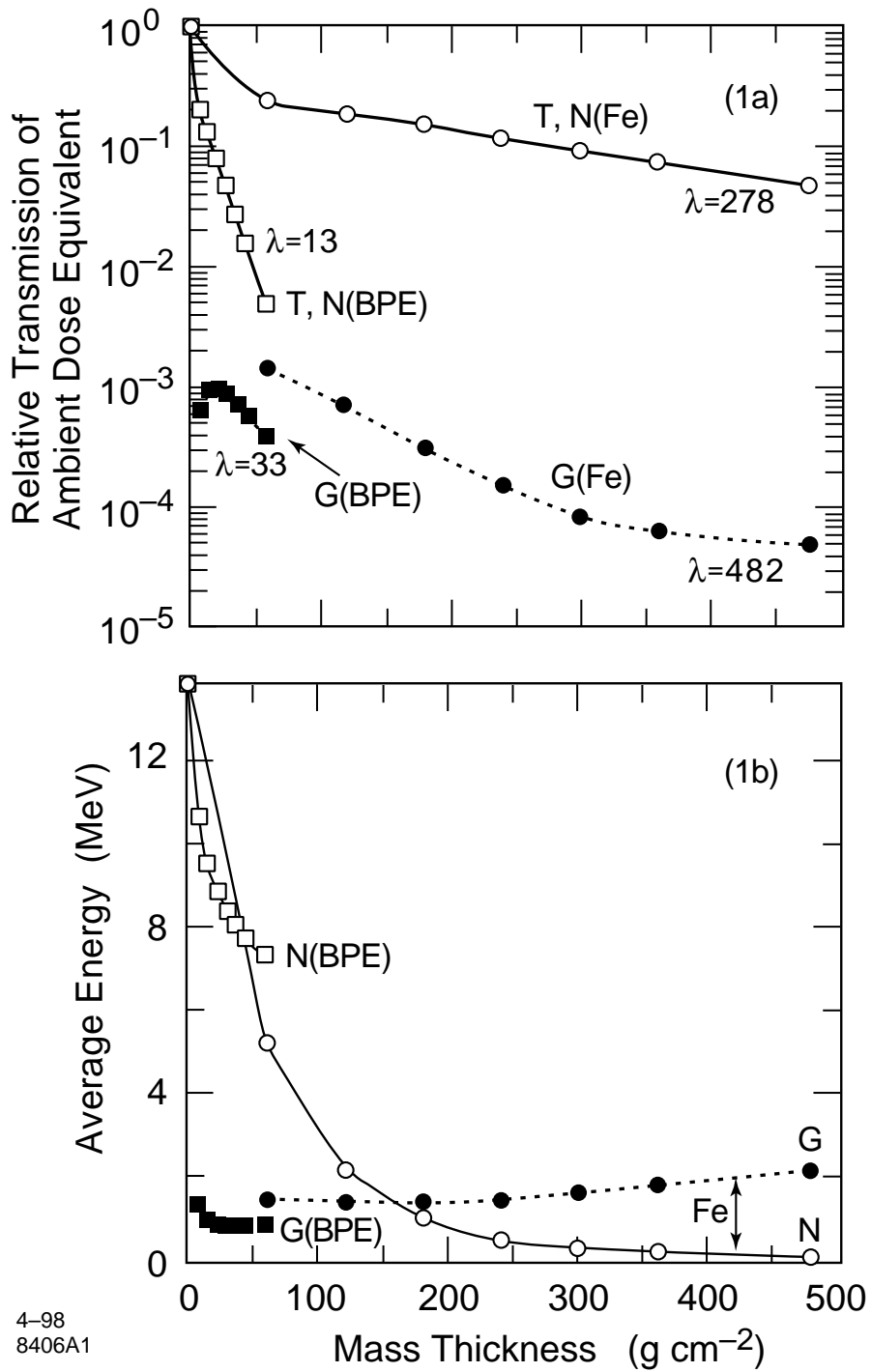
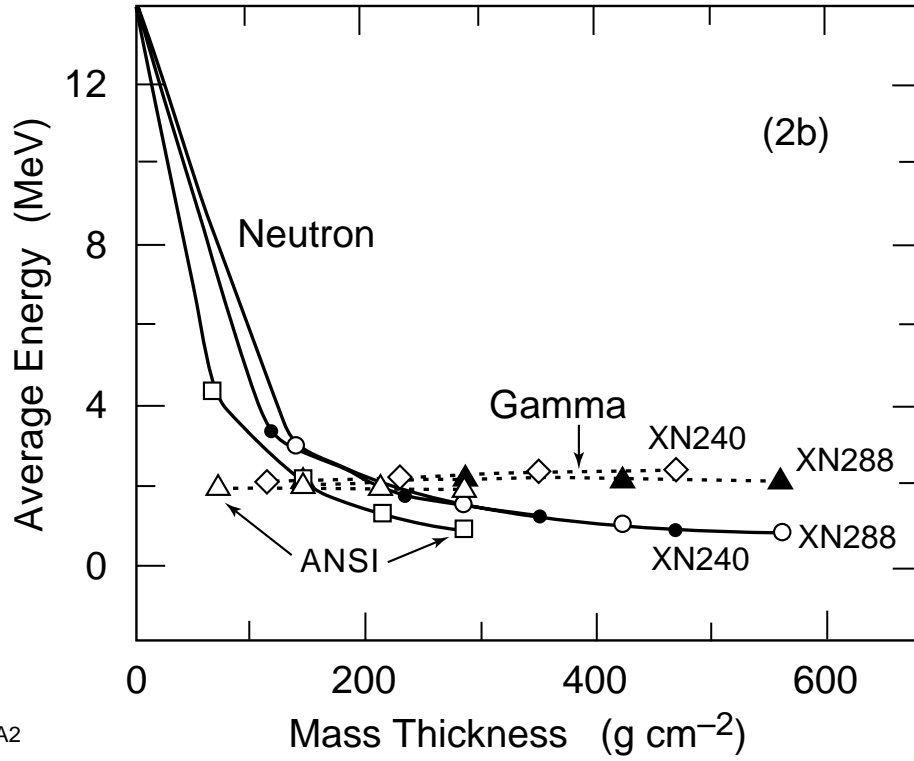
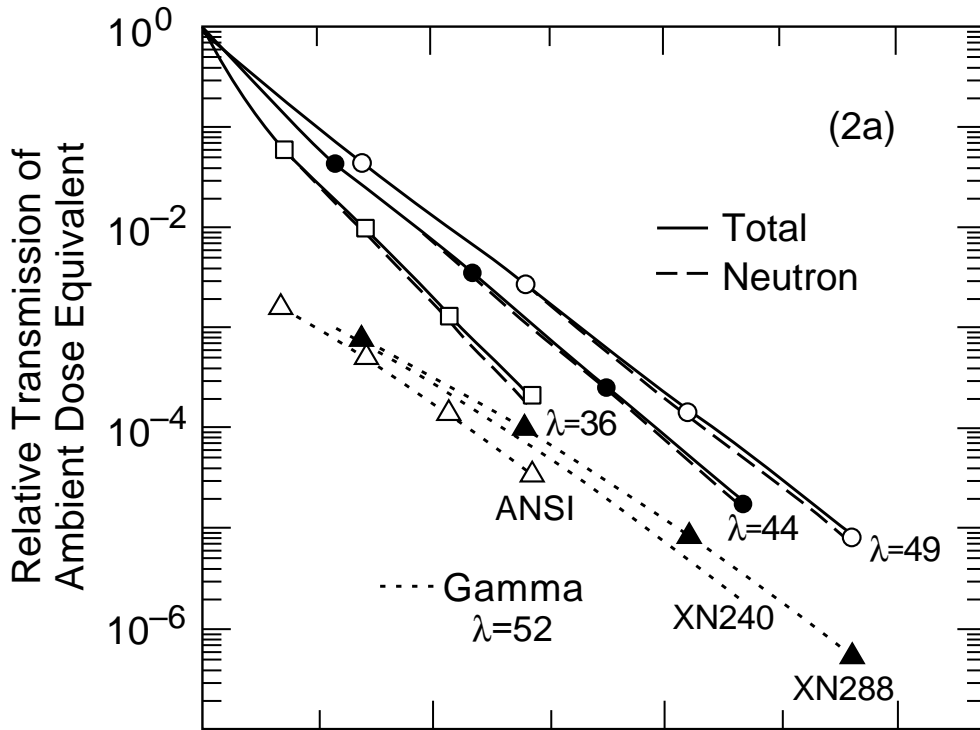


Figure 1. Transmission of ambient dose equivalent (1a) and the resulting average energy (1b) in iron or 10% borated polyethylene (BPE) shield up to 2'-thick. The shield is a spherical shell surrounding a 14-MeV, isotropic neutron source. T: total, N: neutron, G: gamma. The  $\lambda$  value is the neutron or gamma attenuation length in  $g\ cm^{-2}$ .



4-98  
 8406A2

Figure 2. Transmission of ambient dose equivalent (2a) and the resulting average energy (2b) in ANSI concrete and heavy concrete (XN240 and XN288) shield up to 4'-thick. The shield is a spherical shell surrounding a 14-MeV, isotropic neutron source.

Figure 3. Transmission of ambient dose equivalent (3a) and the resulting average energy (3b) in a mixture shield of iron and BPE. The shield is a spherical shell surrounding a 14-MeV, isotropic neutron source. Effects of a 20-cm-thick fluorinert bath surrounding the source on the dose transmission (3a) and on average energy (3c) are also shown.

T: total, N: neutron, G: gamma.

Figure 3a

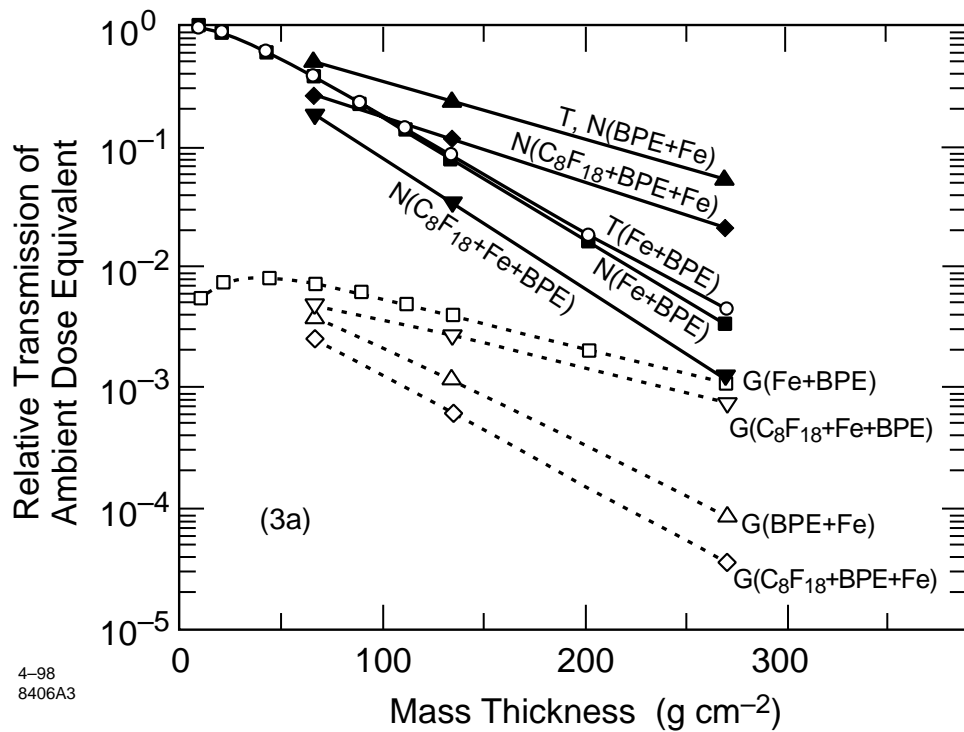




Figure 3b

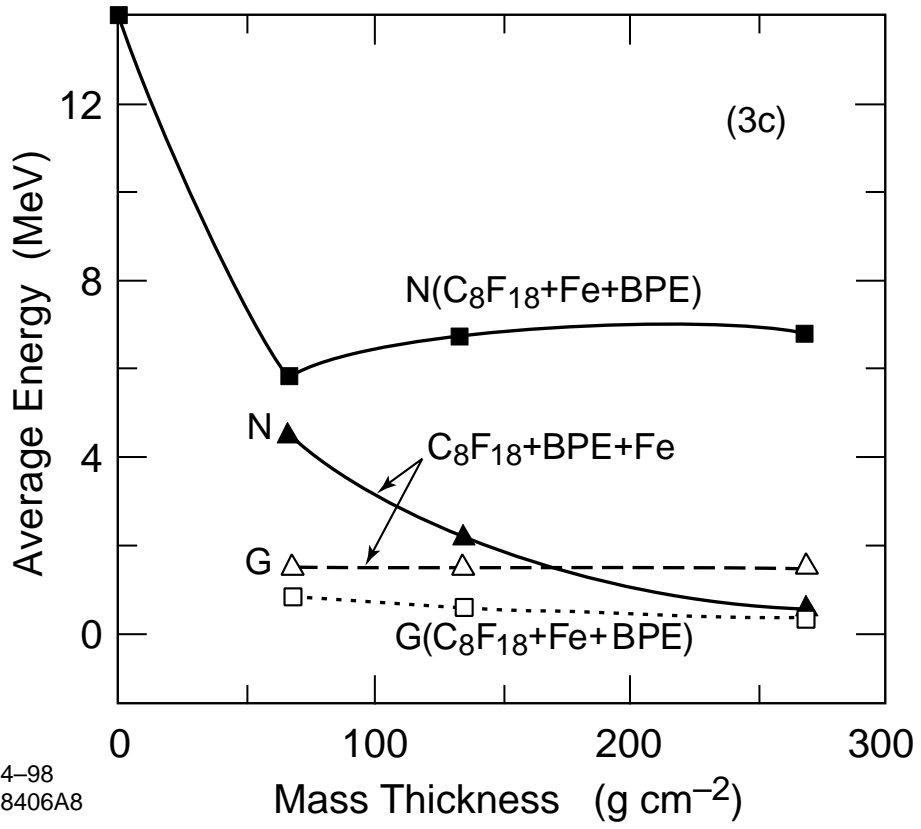
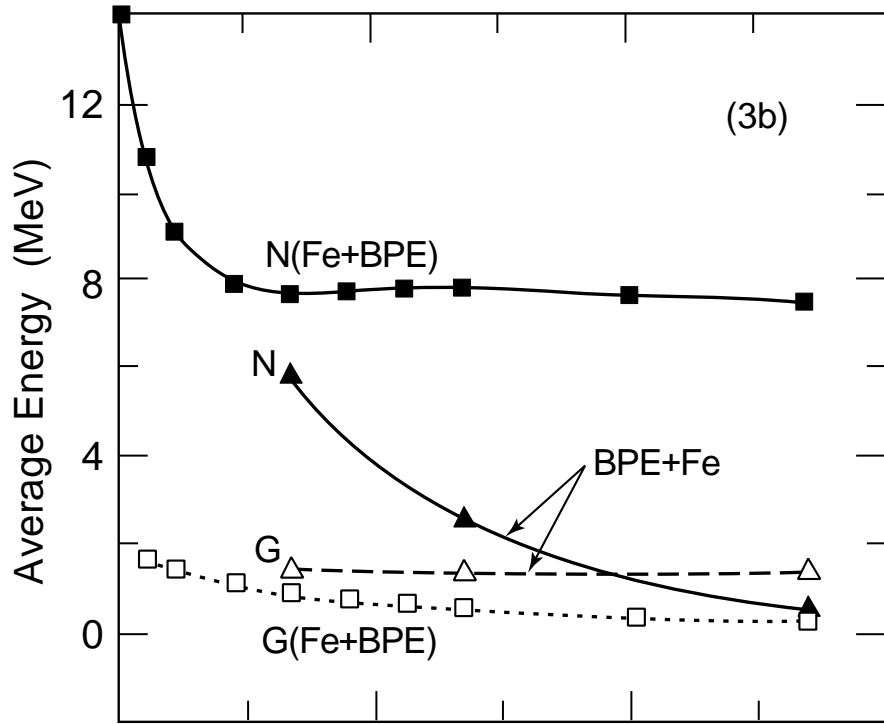
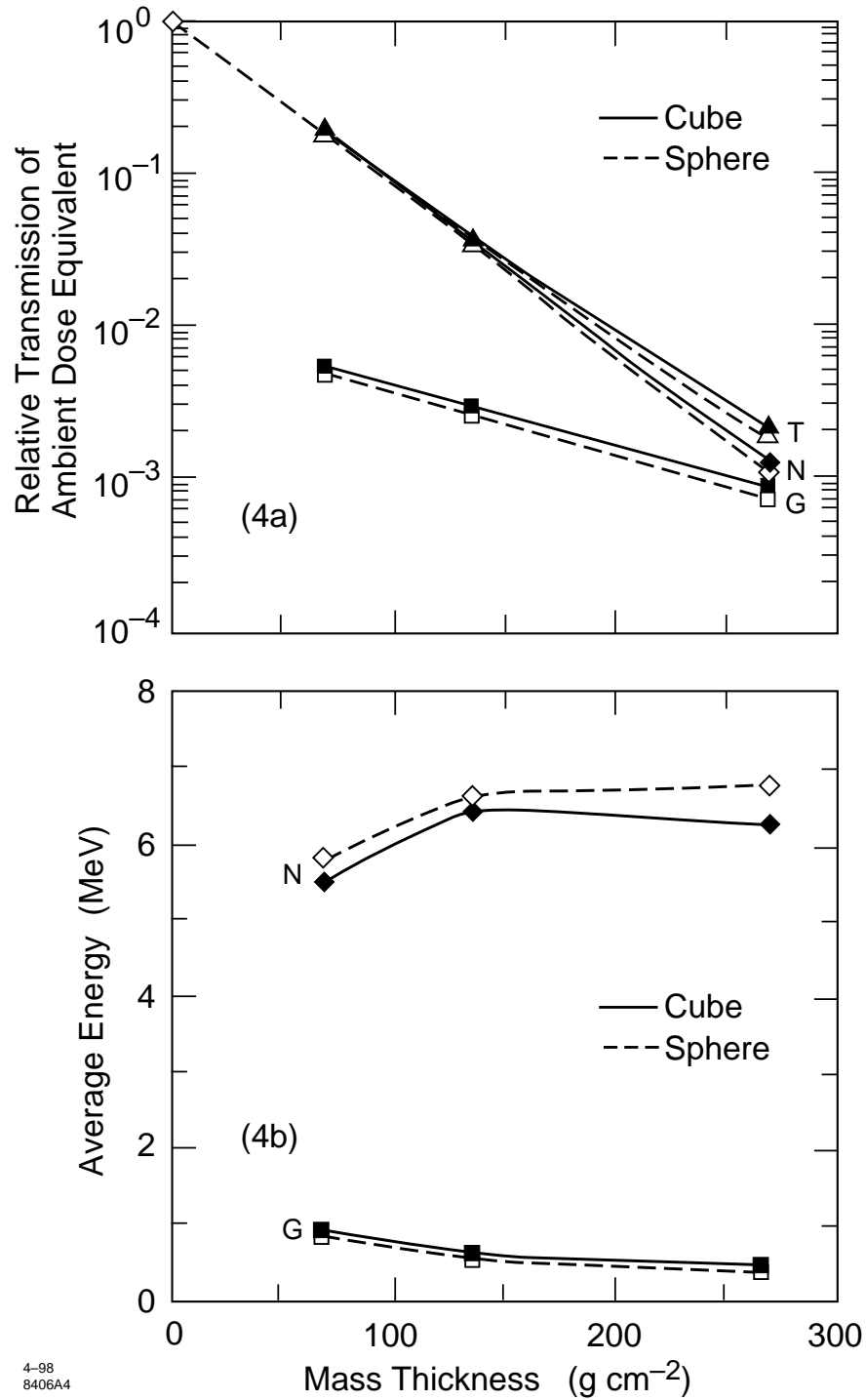


Figure 3c

4-98  
8406A8

Figure 4. A comparison between cubical and spherical shielding geometries: ambient dose equivalent transmission (4a) and average energy (4b). The shield is 20-cm-thick fluorinert followed by iron and BPE. T: total, N: neutron, G: gamma.



4-98  
8406A4

Figure 5. Proposed shielding geometry and dimension in cm (5a). Ambient dose equivalent transmission curves for neutrons (5b), gammas (5c), and total (5d) for detectors D1, D3 and D4. The shield is a fluorinert bath followed by iron and BPE. The surface detector for a spherical shield is shown for comparison.

Figure 5a

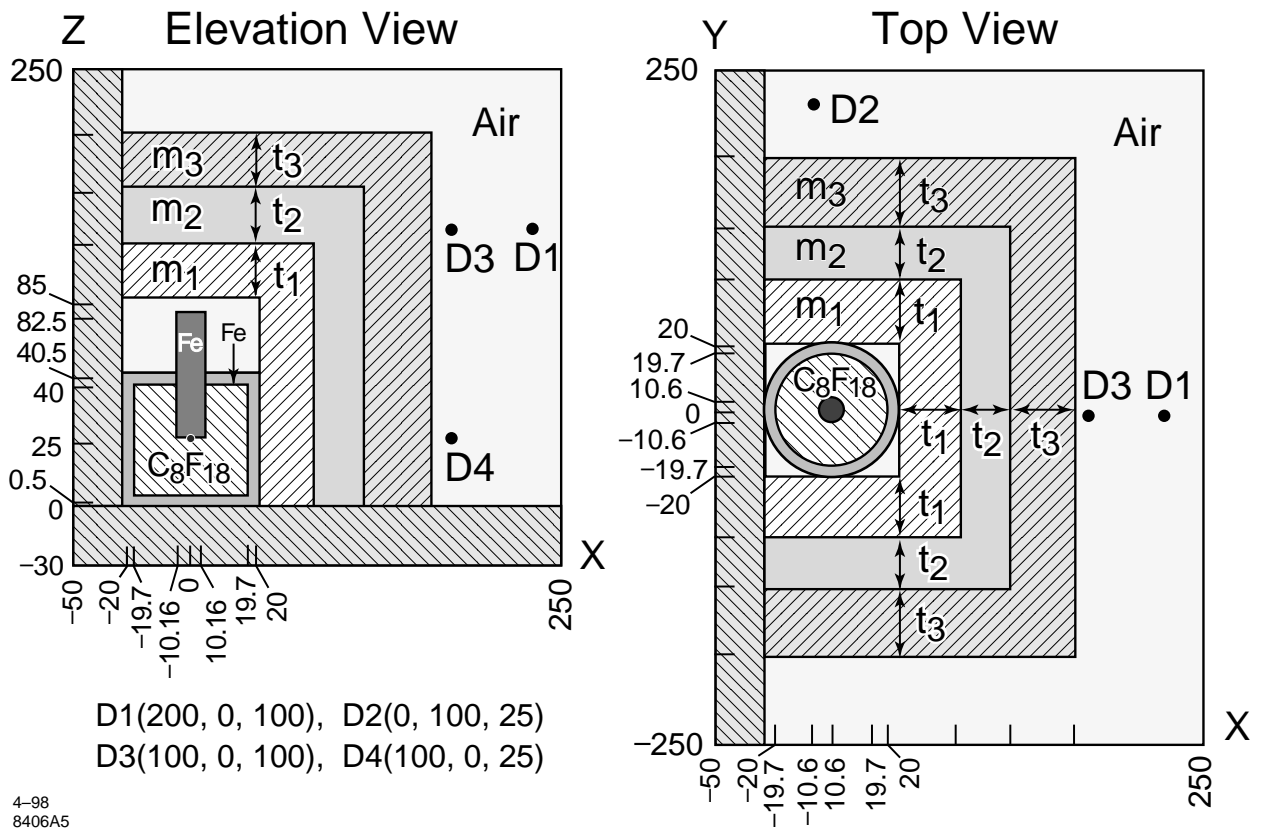


Figure 5b

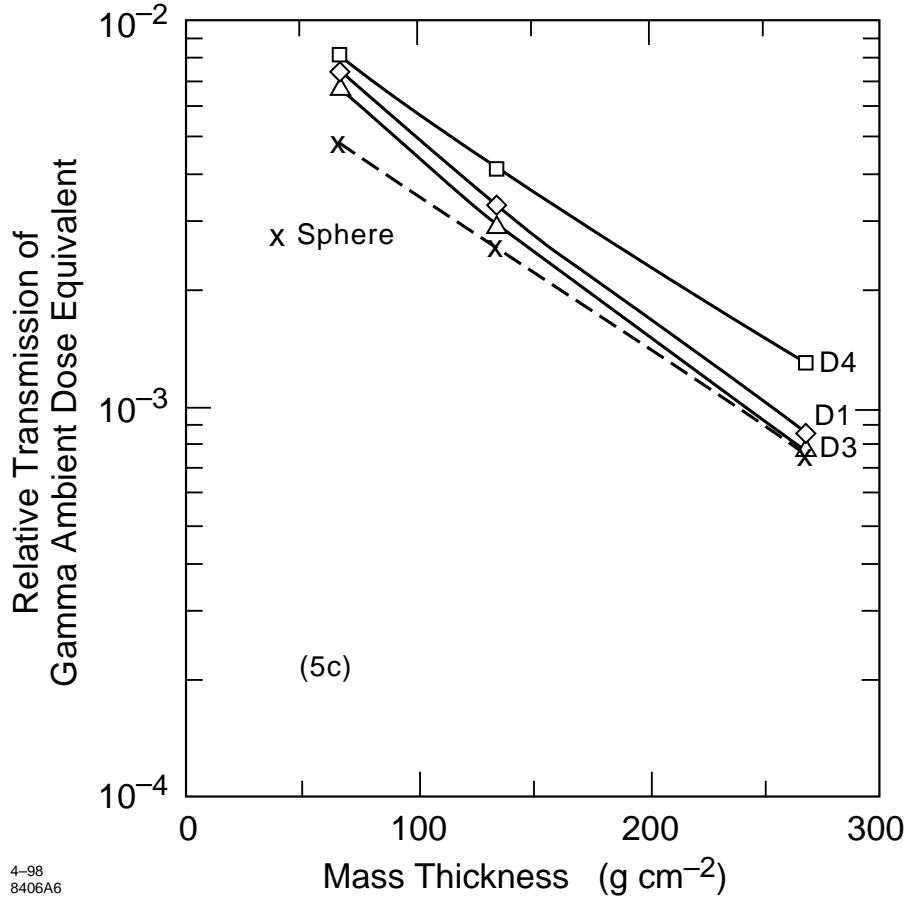
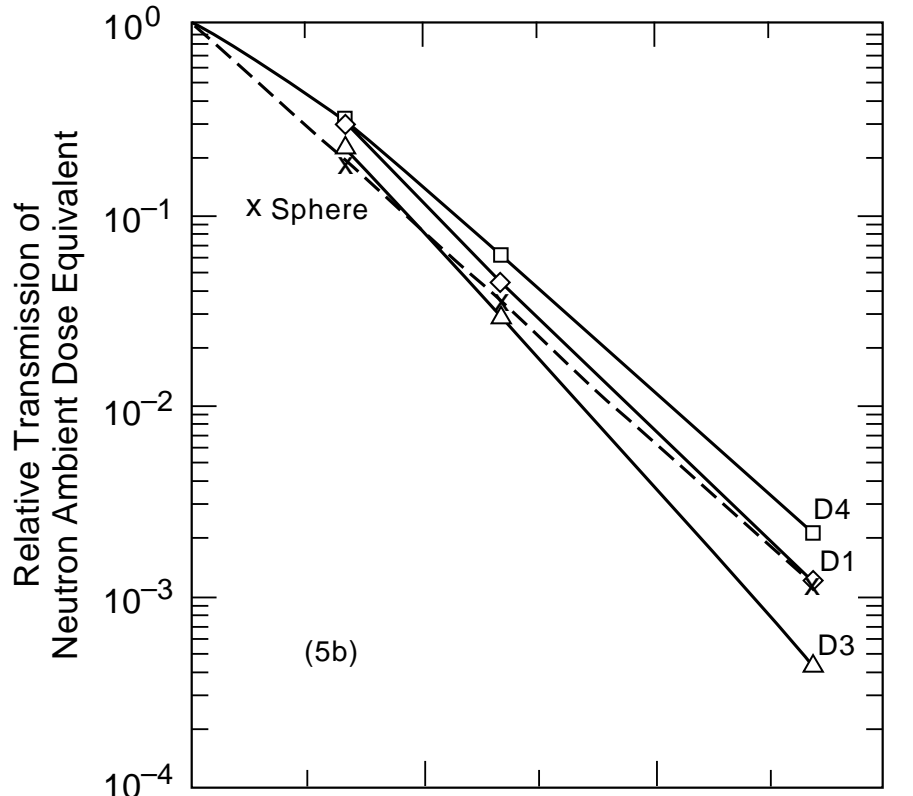


Figure 5c

4-98  
8406A6

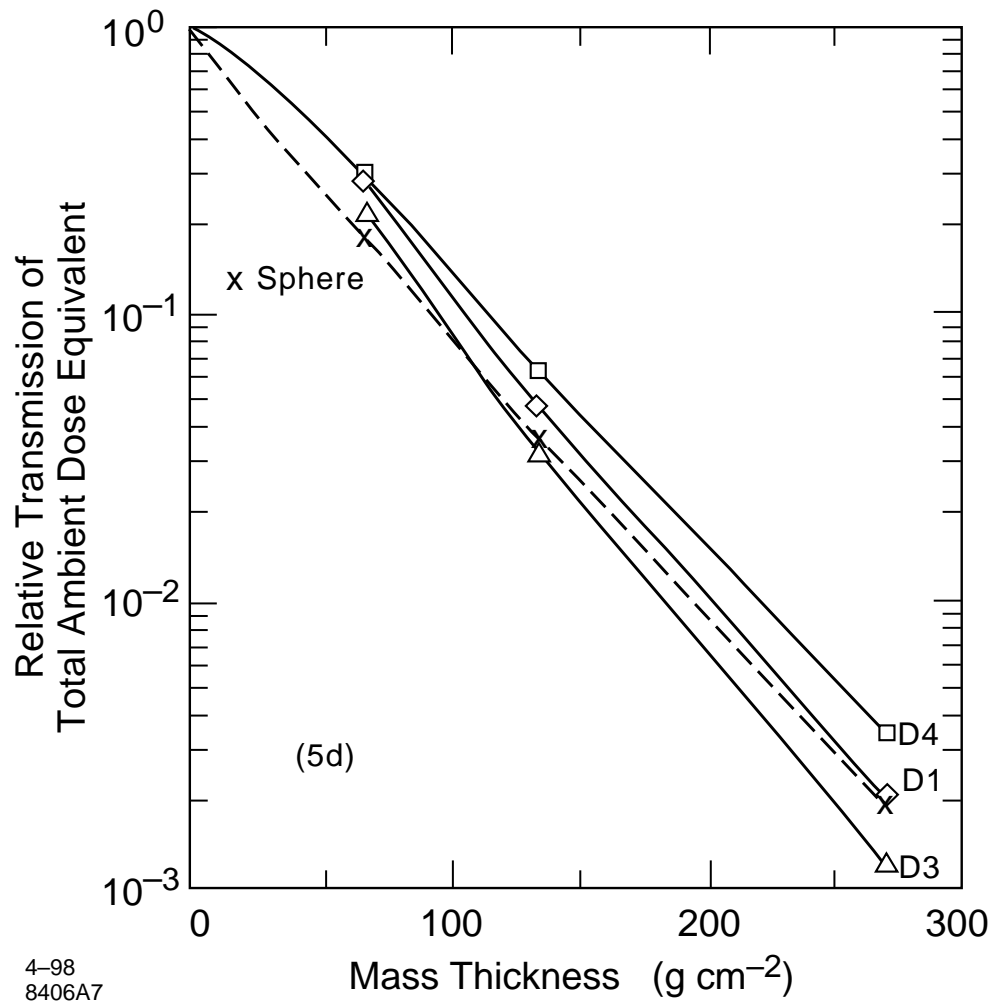


Figure 5d

4-98  
8406A7